

# Simple Hertz-Level Laser Offset Locking by Using a Dual-Bandwidth Digital Band-Pass Filter

Che-Chung Chou<sup>1</sup>, Cheng-Chieh Hsieh, Ko-Han Chen, Yi-Jun Xu, Wang-Yau Cheng, Tyson Lin, and Sheng-Hua Lu<sup>2</sup>

**Abstract**—This letter presents a simple and easy-to-use self-referenced frequency discriminator for laser frequency offset locking. The key component of the “self-referenced” frequency discriminator is a dual bandwidth band-pass filter which is composed of two digital band-pass filters, one having a broader bandwidth to provide a large capture range and the other having a narrow bandwidth for tight frequency locking. The digital band-pass filters are based on the PyRPL IQ modules running on a Red Pitaya STEMLab board. All the parameters of the IQ modules can be easily set and adjusted in the PyRPL GUI. To demonstrate the proposed scheme, we offset locked an external cavity diode laser to an iodine-stabilized external cavity diode laser. Their beat note was narrowed down from 500 kHz of the free running to 4 Hz as offset locked. The minimum Allan deviation of the locked offset frequency is 2.4 Hz at 100-s averaging.

**Index Terms**—Laser frequency offset locking, digital band-pass filter, IQ demodulator, Python Red Pitaya Lockbox.

## I. INTRODUCTION

LASER frequency offset locking is the key technique for transferring optical frequency accuracy from a precisely frequency-stabilized reference laser (RL) to a frequency-tunable slave laser (SL). Because the offset frequency can be precisely controlled, laser frequency offset locking plays an important role in high-resolution laser spectroscopy, laser cooling and trapping, and laser metrology.

Conventionally, a mixer-based system (MBS) is employed where their beat-note signal of the lasers is mixed with a stable RF signal, and then the mixer output is low-pass filtered to serve as the error signal to lock the SL’s frequency. The offset frequency is determined by the RF frequency, while the accuracy of the SL’s frequency can be maintained as that of the ML. Unfortunately, the MBS cannot support a large enough capture range and cannot be applied to lasers with large frequency jitters, a situation particularly severe in the case of diode lasers. Therefore, large capture range techniques are proposed and used, such as the delay-line based offset

locking system [1], [2], band-pass filter based offset locking system (BPS) [3], [4], or using a digital phase and frequency detector [5], [6], [7].

The large capture range will also have less frequency sensitivity at the frequency lock point. To have the ability of having a large capture range and tight frequency locking simultaneously, these large capture range techniques are usually combined with a tight locking scheme, such as MBS [3], [4], [5], [6], external fine-frequency control using AOM [2], or a combination of digital and analog phase frequency detector [5], [6]. As a result, the experiment setups are sophisticated and require more laboratory work.

However, thanks to the well-developed field-programable gate array (FPGA), software-defined instruments have become more easier to deploy in many experiments. For example, Python Red Pitaya Lockbox (PyRPL) [8] is an open source software that allows the use of FPGA boards with analog interfaces to measure and control real-world devices in experiments of atoms, molecules, and optics. In particular, the built-in IQ module of PyRPL can be configured as a digital band-pass filter (DBPF). Therefore, a digital version of BPS can be made. Additionally, the outputs of a wide-bandwidth DBPF can be digitally summed with one of a narrow-bandwidth DBPF to create a dual-bandwidth BPF (DBW-BPF) that can be used to offset lock the lasers with a large capture range and remain a tight locking simultaneously.

In this letter, we report how to offset lock two external cavity semiconductor lasers (ECDLs) to the hertz level by using a DBW-BPF based offset-locking system (DBW-BPS). Compared with using an analog band-pass filter, the benefits of using DBPF are that the offset lock frequency is easy to tune, it has high accuracy, and good temperature stability. The combination of a narrow-bandwidth DBPF with a wide-bandwidth DBPF in the DBW-BPS scheme makes it possible to have a tight locking system for hertz-level stability but still have a broad capture range to prevent the dramatically large frequency jitter.

## II. PRINCIPLE

Fig. 1 shows the schematic diagram of a “self-referenced” frequency discriminator using a DBW-BPF. First, a 90° power splitter divides the beat note  $V_b$  into an in-phase component  $V_{b,i} = A_b \cos(2\pi f_b t)$  for reference and a quadrature component  $V_{b,q} = A_b \sin(2\pi f_b t)$  to feed into the DBW-BPF. Each of the BPFs in the DBW-BPF then filters the quadrature component with the same center frequency  $f_0$ . Due to the different

Received 19 February 2025; revised 22 April 2025; accepted 24 June 2025. Date of publication 27 June 2025; date of current version 3 July 2025. This work was supported in part by Taiwan National Science and Technology Council (NSTC) under Grant 113-2221-E-035-046 and Grant 113-2112-M-008-031. (Corresponding author: Che-Chung Chou.)

Che-Chung Chou, Cheng-Chieh Hsieh, Yi-Jun Xu, Tyson Lin, and Sheng-Hua Lu are with the Department of Photonics, Feng Chia University, Taichung 40724, Taiwan (e-mail: choucc@fcu.edu.tw).

Ko-Han Chen and Wang-Yau Cheng are with the Department of Physics, National Central University, Taoyuan 32001, Taiwan.

Color versions of one or more figures in this letter are available at <https://doi.org/10.1109/LPT.2025.3583756>.

Digital Object Identifier 10.1109/LPT.2025.3583756

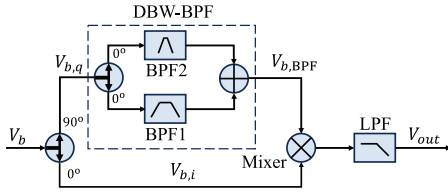


Fig. 1. Scheme of a self-referenced frequency discriminator using a DBW-BPF (dashed line enclosed). BPF: band-pass filter, LPF: low-pass filter. Note that the 90°-power splitter can be removed as discussed in the section of principle.

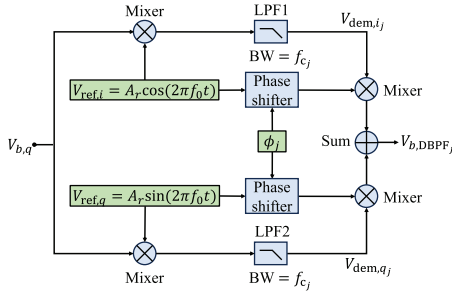


Fig. 2. Schematic of a digital band-pass filter using the IQ module of PyRPL. LPF1 and LPF2 have the same bandwidth value ( $f_{c_j}$ ).

bandwidths of the BPFs, their output signal will have different amplitudes and phase shifts. The output  $V_{b,BPF}$  of the DBW-BPF can be expressed as

$$V_{b,BPF} = \sum_j A_j \sin(2\pi f_b t - \delta_j), \quad j = 1, 2, \quad (1)$$

where  $A_j$  and  $\delta_j$  are the frequency-offset ( $f_b - f_0$ ) dependent amplitudes and phase shifts introduced by each BPF, respectively. The phase shift is an odd function of the frequency offset and, hence, can be used as an error signal for offset lock. To retrieve the phase shift, one can mix  $V_{b,DBWBPf}$  with the in-phase component  $V_{b,i}$  in a mixer and then low-pass filtering the mixer output. The output  $V_{out}$  of a self-referenced frequency discriminator can be shown as

$$V_{out} = -\frac{1}{2} A_b \sum_j A_j \sin \delta_j. \quad (2)$$

The reconfigurable DBPFs made by the PyRPL IQ modules can be used as the BPFs, and the summation can be done by the PyRPL output multiplexer. Fig. 2 is the configuration of the PyRPL IQ module. In the DBW-BPS scheme, the quadrature component  $V_{b,q}$  of the beat note is used as input to the IQ module. For in-phase demodulation in the IQ module,  $V_{b,q}$  is first multiplied with an in-phase reference signal  $V_{ref,i} = A_r \cos(2\pi f_0 t)$  and then filtered by a low-pass filter. The reference signal frequency used in the IQ module determines the  $f_0$  of the DBPF, which is also the offset lock frequency of the DBW-BPS. The low-pass filter cutoff frequency  $f_{c_j}$  determines the half-bandwidth of the  $j$ th DBPF. The complex transfer function  $H_j(f)$  of the first-order low-pass filter can be expressed as

$$H_j(f) = \frac{\exp(-i\delta_j)}{1 + f/f_{c_j}}, \quad (3)$$

where  $f = f_b - f_0$  is the deviation from the offset-locking frequency  $f_0$ , and the phase shift  $\delta_j$  introduced by the low-pass filter can be calculated by using the equation

$$\tan \delta_j = \frac{f}{f_{c_j}}. \quad (4)$$

By multiplying  $V_{b,q}$  with  $V_{ref,i}$ , and then low-pass filtered the result with the transfer function of Eq.(3), the in-phase demodulation  $V_{dem,i}$  is given by

$$V_{dem,i} = \frac{A_b A_r \cos \delta_j}{2 \sqrt{1 + (f/f_{c_j})^2}}. \quad (5)$$

Similarly, the quadrature demodulation  $V_{dem,q}$  is given by

$$V_{dem,q} = \frac{-A_b A_r \sin \delta_j}{2 \sqrt{1 + (f/f_{c_j})^2}}. \quad (6)$$

As shown in Fig. 2, to generate the band-pass filtered output,  $V_{dem,i}$  and  $V_{dem,q}$  are modulated with the  $\phi_j$ -phase-shifted  $V_{ref,i}$  and  $V_{ref,q}$ , respectively. Their results are added together to produce the output  $V_{b,DBPF_j}$ , which can be shown as

$$V_{b,DBPF_j} = \frac{A_b A_r \cos[2\pi f_b t - \delta_j - \phi_j]}{2 \sqrt{1 + (f/f_{c_j})^2}}. \quad (7)$$

Note that the output signal is phase tunable due to the tunable term  $\phi_j$  in Eq. (7). We can satisfy the quadrature condition required in the self-referenced frequency discriminator by adjusting  $\phi_j$  equal to  $\frac{\pi}{2}$  for both DBPFs. Hence, the 90°-power splitter in Fig. 1 can be replaced by the digital multiplex of PyRPL. With fewer passive components, we will benefit from being immune to environmental disturbances, such as the effects of temperature drift on the phase or center frequency and the effect of vibration of the rf cable on the stability of the phase. If one needs to change the offset locking frequency, the small frequency-dependent phase variation of components usually destroys the quadrature condition between the reference beat-note signal  $V_{b,i}$  and the DBW-BPF filtered beat-note signal  $V_{b,BPF}$ . If discrete passive components are used, it is difficult to compensate for this small phase variation. In this scheme, we can easily compensate for the small phase variation by fine-tuning each phase  $\phi_j$  in Eq. (7) to satisfy the quadrature condition for different offset locking frequencies.

After adjusting  $\phi_j$  to satisfy the quadrature condition, the DBPF output signals are summed by the PyRPL output multiplexer. Comparison of the summation of Eq. (7) with Eq. (1), we can find  $A_j$ . Inserting  $A_j$  and  $\sin \delta_j$  back into Eq. (2), the output of a DBW-BPF based self-referenced frequency discriminator can be expressed as

$$V_{out} = \sum_j \frac{-A_b^2 A_r (f/f_{c_j})}{4[1 + (f/f_{c_j})^2]}. \quad (8)$$

We study the frequency response of a single DBPF by plotting, in Fig. 3, the individual term in Eq. (8) with  $f_0$  fixed to 37 MHz for various bandwidths ( $2f_{c_j}$ ). The frequency responses are dispersed, with zero occurring at  $f_0$ , which can be an error signal with a frequency locking point  $f_0$ . As shown in Fig. 3, the response curve of a larger  $2f_{c_j}$  spans a broader frequency

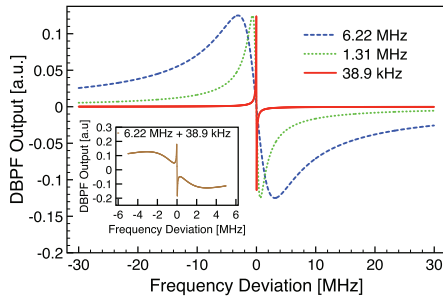


Fig. 3. Theoretical responses of the DBPFs based on PyRPL IQ modules. The zero frequency deviation is the DBPF band-center frequency. The DBPFs are centered at 37 MHz and have bandwidths of 6.22 MHz (blue dashed line), 1.31 MHz (green center line), and 38.9 kHz (orange solid line). The inset shows the response curve of a DBW-BPF with a combination bandwidth of 38.9 kHz and 6.22 MHz.

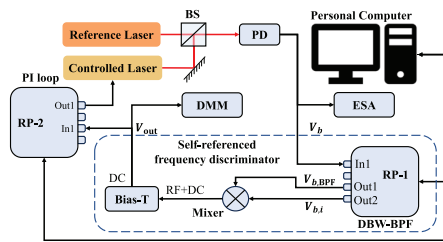


Fig. 4. Experiment setup of the DBW-BPF based offset lock system. BS: beam splitter, PD: photodetector (Bandwidth: 1 GHz), ESA: electrical spectrum analyzer, DMM: digital multimeter, RPs: Red Pitaya STEMLab 125-14 boards (Input ADC: 60 MHz, 14-bit for  $\pm 1$ -V).

range, while that of a smaller  $2f_c$  has a steeper slope near  $f_0$ . In the DBW-BPS scheme, the output of two DBPFs with one smaller  $2f_c$  and one large  $2f_c$  is summed to produce a hybrid frequency response, such as shown in the inset of Fig. 3. In this way, the DBW-BPS is able to capture the SL with a large de-tuning to  $f_0$ . As the SL is captured and pulled toward  $f_0$ , the DWB-BPS automatically turns the offset lock into a tighter lock due to the steeper slope near  $f_0$ . Furthermore, while the SL is offset locked, any dramatically large frequency jitters that cause the frequency to jump outside the steeper slope can be re-locked automatically by the response contributed from the DBPF with larger bandwidth.

### III. EXPERIMENT SETUP

The experimental setup shown in Fig. 4 is built to implement the concept of DBW-BPS. Both the ML and the SL are homemade 1079-nm ECDLs. The second harmonic of the ML is frequency stabilized to the  $a_1$  component of the R (81)29-0 transition of iodine near 540 nm. More details of the lasers can be found in [9]. The beat-note signal  $V_b$  is generated by a photodetector (PD), and its spectrum is monitored by an electrical spectrum analyzer (ESA).  $V_b$  is sent to the self-referenced frequency discriminator (the dashed-line blocked region in Fig. 4). The discriminator output  $V_{out}$ , monitored by a digital multimeter (DMM), acts as an error signal and is sent to a proportional integration loop filter (PI loop) to close the offset-lock feedback loop. In this work, we use one of the PyRPL PI modules to be the PI loop for current-feedback

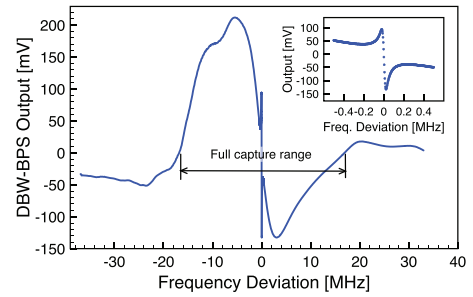


Fig. 5. Frequency response of an DBW-BPS. The zero frequency deviation is the band-center frequency. Two DBPFs centered at 37 MHz with bandwidths of 6.22 MHz and 38.9 kHz were used.

control of the SL. Since PyRPL runs exclusively on Red Pitaya [10], we used two Red Pitaya STEMLab 125-14 boards (RPs) to run the PyRPL IQ and PI modules separately.

Inside the self-referenced frequency discriminator, two PyRPL IQ modules running on the RP-1 with different  $f_c$  are used to build the two DBPFs of the DBW-BPF. The phase shift  $\phi_j$  of each IQ module shall be adjusted separately to ensure zero response at the center frequency, which is equivalent to ensuring the quadrature relationship between  $V_{b,BPF}$  and  $V_{b,i}$ . Note that there is an extra propagation phase delay inside RP. To compensate for this extra delay, the in-phase component  $V_{b,i}$  is also sent to the third PyRPL IQ module. However, the low-pass filter of the third IQ module is turned off to pass the in-phase component without any filtering effect. The three IQ modules are set with the same  $f_0$ . The settings of the IQ modules were all done in the PyRPL GUI. Note that the thermal stability of  $f_0$  is determined mainly by the clock of RP (1 ppm/ $^{\circ}$ C).  $V_{b,BPF}$  and delayed  $V_{b,i}$  are output from the two RF outputs of RP-1, and then mixed by a mixer (Mini Circuit ZAD-1+). At the output end of the self-referenced frequency discriminator, we used the DC port of a bias-T (Mini Circuit ZFBT-4R2GW+) to replace a low-pass filter. By the way, the rf output from the bias-T can also be used to monitor the second harmonic of the beat note. The  $V_{out}$  of the self-referenced frequency discriminator is served as an error signal and sent to the PyRPL PI loop running on RP-2.

### IV. RESULTS

We used a frequency-scanned RF signal to test the frequency response of DBW-BPS based on the PyRPL IQ modules. A typical frequency response of  $V_{out}$  recorded by DMM is shown in Fig. 5. The response near  $f_0$  shows a very steep slope similar to that in the inset of Fig. 3. We also observe that decreasing  $f_0$  will increase the strength of the frequency response. As we will show later, the SL can be well offset-locked with 37 MHz. This implies that  $f_0$  can be tuned to any value less than 37 MHz, which is more than eight times the tuning range of the analog band-pass filter used in [4]. Compared to the inset of Fig. 3, Fig. 5 shows a narrower signal cutoff on the upper edge, which might be due to the 60-MHz bandwidth limit of RP. Estimated from the zero crossings other than  $f_0$  in Fig. 5, the full capture range is about 34 MHz.

As shown in Fig. 6 (a), before the PI loop was closed, the beat-note spectrum measured by ESA was centered at 58 MHz

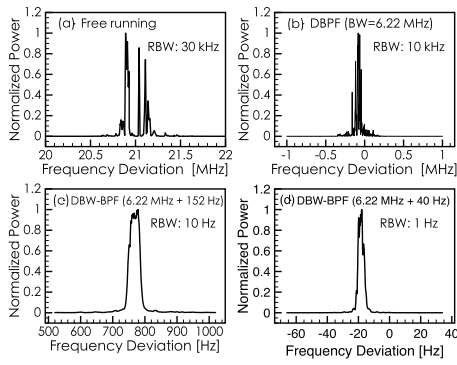


Fig. 6. The beat-note electrical spectra (a) before and (b), (c), (d) after the PI loop is closed. The resolution bandwidth (RBW) of the ESA is shown in each plot. The bandwidth of DBPF or DBW-BPF is (b) 6.22 MHz, (c) 6.22 MHz + 152 Hz, (d) 6.22 MHz + 40 Hz. The zero frequency deviation is the band-center frequency (37 MHz) of the DBPF or DBW-BPF.

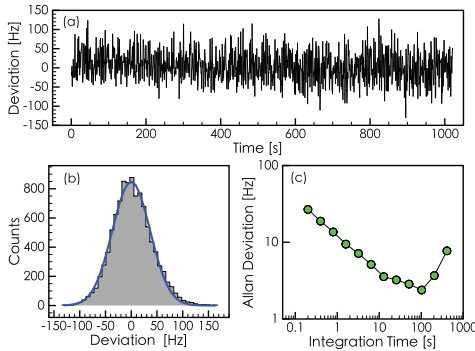


Fig. 7. Offset-locked beat-note frequency stability using a DBW-BPF with combination bandwidths of 6.22 MHz + 40 Hz. (a) Residual offset frequency fluctuation relative to  $f_0$  measured by a counter (Keysight 53220A counter at 10 samples/s). (b) Histogram of (a), (c) Allan deviation of (a).

and spanned over 500 kHz. With a single DBPF of 6.22-MHz bandwidth, the beat frequency can be captured and pulled close to  $f_0$  (37 MHz) with a deviation of 0.1 MHz, as shown in Fig. 6 (b). While the offset frequency is captured and locked, another smaller bandwidth DBPF can be turned on to make a DBW-BPS to tightly lock the offset frequency. As shown in Figs. 6 (c) and (d), with the larger bandwidth fixed, the beat-note spectrum was pulled closer to  $f_0$  and became narrower as the smaller bandwidth decreased. The smallest bandwidth for stable offset locking of our lasers is 40 Hz (Fig. 6 (d)) where the beat-note spectrum was narrowed down to 4 Hz with an 18-Hz frequency deviation. We also observed a frequency drift of 20 mHz/s. The deviation or drift can be reduced by an active control of  $\phi_j$  with the SL locked. Compared to the analog BPS scheme, where an additional LC tuning circuit is added [4], this can be done by using the PyRPL API.

Fig. 7 (a) shows a 17-min. residual offset frequency relative to 37 MHz  $f_0$ . The corresponding histogram is plotted in Fig. 7 (b) and is well fitted to a Gaussian distribution with a standard deviation of 43 Hz. The Allan deviations of the 17 min. residual offset frequency at various averaging times is shown in Fig. 7(c). The minimum frequency stability is 2.4 Hz with a 100-s averaging time. We find a similar behavior of

the Allan deviation as the beat note is replaced by a free-running signal generated by the PyRPL ASG module. Hence, we conclude that the minimum stability occurring at 100 s averaging time is limited by the frequency drift of the RP onboard clock. To further improve the frequency stability, we suggest that the RP external clock model should be used.

## V. CONCLUSION

In conclusion, we demonstrate a simple and easy-to-use dual-bandwidth BPS scheme for laser frequency offset locking capable of a large capture range (several ten megahertz) and a tight locking (hertz level). The key component of this offset locking system is a dual-bandwidth BPF composed of two DBPFs with one broader bandwidth and one narrow bandwidth, which are based on the PyRPL IQ modules and are easy to reconfigure. Using this scheme, we successfully offset lock two home-made ECDLs with a hertz-level uncertainty for 100 s-averaging. Further improvement in long-term stability can be achieved by using a stable external clock to replace the internal clock of the RP or active control of  $\phi_j$ .

## ACKNOWLEDGMENT

The authors would like to thank Prof. Jow-Tsong Shy for the helpful advice.

## REFERENCES

- [1] U. Schünemann, H. Engler, R. Grimm, M. Weidemüller, and M. Zielonkowski, "Simple scheme for tunable frequency offset locking of two lasers," *Rev. Sci. Instrum.*, vol. 70, no. 1, pp. 242–243, Jan. 1999. [Online]. Available: <http://scitation.aip.org/content/aip/journal/rsi/70/1/10.1063/1.1149573>
- [2] X. Chen, Q. Liu, Y. Wang, F. Meng, and B. Luo, "A high-precision offset frequency locking technique with delay line reference and AOM-based compensation," *IEEE Photon. J.*, vol. 13, no. 4, pp. 1–6, Aug. 2021. [Online]. Available: <https://ieeexplore.ieee.org/document/9511311/>
- [3] W.-Y. Cheng, T.-J. Chen, C.-W. Lin, B.-W. Chen, Y.-P. Yang, and H. Y. Hsu, "Robust sub-millihertz-level offset locking for transferring optical frequency accuracy and for atomic two-photon spectroscopy," *Opt. Exp.*, vol. 25, no. 3, pp. 2752–2762, Feb. 2017. [Online]. Available: <https://www.osapublishing.org/abstract.cfm?URI=oe-25-3-2752>
- [4] Y. Seishu and T. Hasegawa, "Robust offset locking of laser frequency with electronically tunable LC circuits for sub-millihertz uncertainty," *Appl. Phys. B, Lasers Opt.*, vol. 125, no. 8, p. 142, Aug. 2019, doi: [10.1007/s00340-019-7253-5](https://doi.org/10.1007/s00340-019-7253-5).
- [5] N. Beverini, M. Prevedelli, F. Sorrentino, B. Nyushkov, and A. Ruffini, "An analog+digital phase-frequency detector for phase locking of a diode laser to an optical frequency comb," *Quantum Electron.*, vol. 34, no. 6, pp. 559–564, Jun. 2004, doi: [10.1070/qe2004v034n06abeh002655](https://doi.org/10.1070/qe2004v034n06abeh002655).
- [6] J. Appel, A. MacRae, and A. I. Lvovsky, "A versatile digital GHz phase lock for external cavity diode lasers," *Meas. Sci. Technol.*, vol. 20, no. 5, May 2009, Art. no. 055302, doi: [10.1088/0957-0233/20/5/055302](https://doi.org/10.1088/0957-0233/20/5/055302).
- [7] Z. Xu, X. Zhang, K. Huang, and X. Lu, "A digital optical phase-locked loop for diode lasers based on field programmable gate array," *Rev. Sci. Instrum.*, vol. 83, no. 9, Sep. 2012, Art. no. 093104, doi: [10.1063/1.4750143](https://doi.org/10.1063/1.4750143).
- [8] L. Neuhaus et al., "Python red pitaya lockbox (PyRPL): An open source software package for digital feedback control in quantum optics experiments," *Rev. Sci. Instrum.*, vol. 95, no. 3, Mar. 2024, Art. no. 033003. [Online]. Available: <https://pubs.aip.org/rsi/article/95/3/033003/3269904/Python-Red-Pitaya-Lockbox-PyRPL-An-open-source>
- [9] K.-H. Chen, "A proposal and demonstration on setting up laser power standard via atom system," Ph.D. dissertation, Dept. Phys., Nat. Central Univ., Taoyuan, Taiwan, 2025.
- [10] (May 2021). *Red Pitaya-Swiss Army Knife For Engineers*. [Online]. Available: <https://redpitaya.com/>